Histopathological and Biochemical Changes in Acute and Chronic toxicity of Strox; A Psychoative Substance in Egypt

Salma I. Abdelkader[1], Asmaa A. Abo Zeid[2], Walaa Baher[2], Shimaa Talaat[3], Rania Hussien[1]

KEYWORDS
Strox;
Toxicity;
Designer drugs;
Synthetic cannabinoids.

ABSTRACT

Strox is an Egyptian version of spice. It is a mixture of several substances sprayed on the plant to enhance its effect. This study aimed to assess the histopathological and biochemical effects of Strox after acute and chronic exposure through an experimental approach. We classified eighty adult male Wistar rats into four groups: a negative and positive control group, an acute toxicity group that received 1/3, 2/3, and LD50, respectively, and a chronic (dependence) group. The biochemical analysis included aspartate aminotransferase (AST), alanine transaminase (ALT), serum urea, creatinine, creatine phosphokinase (CPK), Creatine Kinase-MB (CK-MB), and troponin in addition to histopathological examination of the cerebellum, heart, lung, liver, and kidney. There was a significant increase in AST, ALT, total CPK, and CK-MB in the dependence group. Up until the loss of hepatocytes, there was a tremendous affection for hepatocytes in both acute and chronic groups. Cardiac muscles showed necrosis and fragmentation in both groups. In both groups, the kidneys showed renal tubular necrosis. In both groups, the cerebellum exhibited distortion and a decrease in the number of stellate, basket, and Purkinje cells. In all experimental groups, the lung showed thickened alveolar septa with inflammatory cells and hemorrhage. The study concluded that acute and chronic Strox toxicity induced profound histopathological changes in the heart, lung, liver, cerebellum, and kidney. These changes were further confirmed by the altered biochemical tests in the chronic group.

Introduction

The term "designer drugs" refers to substances obtained through a surreptitious modification of known substances of abuse, preserving or enhancing pharmacologic action while remaining outside legal control**.** Currently, Luethi and Liechti (2020) apply the term more broadly to substances that originate from industry or academic research but never receive medical approval.

Synthetic cannabinoids (SC) are one of the designer drugs that emerged rapidly. People sell them in various forms, such as "herbal blends," "incense," or "spice products." They are readily available through smoke shops and the internet. Moreover, they usually escape laws and regulations by labeling it as “not for human consumption” (Wilson et al., 2016).

The Strox is an Egyptian version of the Spice, also known as Vodoo, and people use both names interchangeably. It consists of a mixture of several substances, such as anticholinergics (Atropa belladonna, Datura, or Hyoscyamus), CNS stimulants (methylene dioxymethamphetamine (MDMA), and many other active substances that could be used as a plant mixture after spraying to enhance its

(1) Forensic Medicine and Clinical Toxicology Department, Faculty of Medicine, Ain Shams University, Cairo, Egypt
(2) Histology and Cell Biology Department, Faculty of Medicine, Ain Shams University, Cairo, Egypt
(3) Fellow of Biochemistry, Poison control center, Ain Shams University Hospitals, Cairo, Egypt

effect. Interestingly, clandestine laboratories could use innocent plants as a matrix for manufacturing Strox after adding significant amounts of active substances (Sobh et al., 2018; El-Masry and Abdelkader, 2021).

So, comprehensive studies are required to assess the impact of this substance, "Strox," on the structure and biological functions of various organs to correlate it with the clinical picture observed in patients presented with acute and chronic toxicity to help in their management for a better prognosis.

Therefore, this study aims to assess the histopathological and biochemical effects of Strox after acute and chronic exposure.

Material and Methods

The Medical Research Center at Ain Shams University (MASRI) conducted this experimental study. The study included groups of adult male Wistar albino rats. The institutional ethical committee of the Faculty of Medicine, Ain Sham University, approved the study (No. FMASU R67/2018), ensuring it complied with the ARRIVE guidelines.

Declarations

We affirm that we performed all methods in compliance with the applicable guidelines and regulations.

The sample size was calculated using the equation E= (total number of animals - total number of groups), where E shouldn't be less than 10. Taking into account the 29% attrition rate, we found that a sample size of at least 64 male albino rates split into 8 groups with 8 rates in each group was enough to meet the study's goals (Charan and Kantharia, 2013).

Chemicals

Patients who visited the Poison Control Center of Ain Shams University (PCC-ASU) provided the seized Strox sachets. Each Strox sachet contains 3 grams**.** It was filled with dried, crushed green herbal material.

Extract preparation:

Strox extract was prepared by crushing the herbal material in the sachets. Every 3 grams were extracted three times with an equal mixture of diethyl ether and light petroleum (40-60) then after the third time of extraction, the solution was filtered using a micro-filter.

Time and route of administration:

Each animal in the acute toxicity group received one intraperitoneal dose of Strox extract, while the chronic (dependence) group received gradually increasing doses for one month.

Dose:

The dose of Strox extract was calculated according to the LD_{50} (1334 mg/kg) in rats according to Abass et al. (2017).

The animals

For this experiment, researchers selected 80 adult male albino rats with an average weight of 150–200 g at the start of the study and housed them in cages with controlled temperatures and humidity.

We left all rats in their housing for 2 weeks before conducting the experiment to allow them to adapt to the environmental conditions. During this period, animals received a balanced diet containing essential elements and vitamins. We supplied clean containers with tap water throughout the experiment.

Experimental Design:

We randomly divided the rats into the following groups: We generated random numbers using Microsoft Excel's standard = RAND function.

Group (I) (negative control group): This group consisted of 20 rats, divided into two groups of 10 rats each.

- **The sub-group (IA)** rats were kept in the cages without any handling for the same period as the rats in group III (acute toxicity group) to determine the normal histological findings.
- **Sub-group (IB)** rats were kept in the cages without any handling for one month as the rats of group IV (dependence group) to determine the normal histological findings.

Group (II) (Positive control group): The animals of this group received the vehicle only ethyl ether. They consisted of 20 rats, divided into two groups of 10 rats each.

- **Sub-group (IIA):** Intraperitoneal (IP) administration of 1 ml of diethyl ether; the vehicle of the extract once as the rats of group III (acute toxicity group).
- **Sub-group (IIB):** Intraperitoneal (IP) administration of 1 ml of diethyl ether; the vehicle of the extract daily for one month as the rats of group IV (dependence group).

Group (III) (Acute toxicity group): This group consisted of 30 rats, which were further divided into 3 groups of 10 rats each.

- **Sub-group (IIIA):** Received 444.66 mg/kg (1/3 LD50 of Strox extract) once.
- **Sub-group (IIIB**): Received 889.33 mg/kg (2/3 LD50 of Strox extract) once.
- **Subgroup (IIIC):** Received 1334 mg/kg (LD50 of Strox extract) once.

Group (IV) (Dependence group): We administered a gradually increasing IP dose of Strox extract to 10 rats. Initially, each animal received 1/10 of the LD50 (133.4 mg/kg/day) for the first 10 days, followed by a doubled dose of 266.8 mg/kg/day (1/5 LD50) between 11–20 days, and a final dose of four times the initial dose (533.6 mg/kg/day) between 21–30 days.

Biochemical analysis

At the end of the experiment, we collected three milliliters of blood from each animal. We centrifuged the collected samples at 4000 g for 10 minutes**.** We used the Cobas Integra Sys system (Roche Diagnostics, Mannheim, Germany) to determine serum aspartate aminotransferase (AST), alanine aminotransferase (ALT), serum creatinine, serum urea, total creatine phosphokinase (CPK), creatine kinase-MB (CK-MB), and cardiac troponin levels through kinetic and kinetic Jaffe reactions.

Histopathological examination

After euthanizing the animals at the end of the experiment, we rapidly dissected and excised the cerebellum, heart, lung, liver, and kidney, rinsed them in saline solution, and cut them into 1-2 cm3 pieces. We then fixed these pieces in neutral buffered formaldehyde solution (10%) for a minimum of 48 hours before embedding them in paraffin wax. We mounted sections of 5 microns thick on glass slides, stained them with hematoxylin and

eosin (Hx & Ex) following Drury & Wallington's (1980) method, and examined them under a light microscope for histopathological investigation.

Statistical analysis

Biochemical data were collected, revised, coded, and entered into the Statistical Package for Social Science (IBM SPSS) version 23. The quantitative parametric data were presented as mean, standard deviations, and ranges. The comparison between more than two groups with quantitative parametric data was done by using the One Way ANOVA test followed by post hoc analysis using the LSD test when significant. The confidence interval was set to 95% and the margin of error accepted was set to 5%. Therefore, the p-value was deemed significant as follows**:** So, the p-value was considered significant as the following: $P > 0.05$: Non significant (NS), $P < 0.05$: Significant (S), and $P < 0.01$: Highly significant (HS).

Results

There was a significant increase in the levels of both AST and ALT in the dependence group (group IV) compared to the negative and positive control groups (Tables 1, 2). The kidney function tests (serum urea and creatinine) showed no significant difference between the groups (Table 3). In terms of the total CPK and CK-MB, there was a significant increase in their levels in the dependence group compared to both negative and positive control groups, but the troponin level was negative in all compared groups (Tables 4, 5).

Table (1): One way ANOVA to compare liver enzymes (ALT and AST) among groups (IB), (IV) and (IIB)

		Group (IB)	Group (IV)	Group (IIB)	Test value•	P-value	Sig.
		n = 10	n = 10	n = 10			
AST (U/L)	Mean ± SD	32.50 ± 3.66	134.00 ± 14.70	39.60 ± 6.11	361.065	0.000	HS
	Range	28 – 39	113 – 156	26 – 49			
ALT (U/L)	Mean ± SD	25.40 ± 1.71	32.90 ± 4.58	26.70 ± 1.77	17.819	0.000	HS
	Range	23 – 28	27 – 41	24 – 29			

Group (IB): (Negative Control group), Group (IIB): (Positive control group), Group (IV): (dependence group), SD: standard deviation; P-value >0.05: Non significant (NS); P-value <0.05: Significant (S); P-value< 0.01: highly significant (HS); n= number; AST: Aspartate transaminase; ALT: Alanine transaminase, •: One Way ANOVA test

Table (2): Post hoc statistical analysis to compare between three groups (negative IB and positive control IIB) versus dependence group (IV) as regards liver enzymes

	Post Hoc analysis by LSD		
	Group (IB) Vs Group (IV)	Group (IB) Vs Group (IIB)	Group (IIB) Vs Group (IV)
AST	0.000	0.104	0.000
ALT	0.000	0.342	0.000

Group (IB): (Negative Control group), Group (IIB): (Positive control group), Group (IV): (dependence group), LSD: least significant difference, P-value >0.05: Non significant, P-value <0.05: Significant, P-value< 0.01: highly significant, Vs: versus, AST: Aspartate transaminase; ALT: Alanine transaminase

Table (3): One way ANOVA to compare kidney function test (S. urea and creatinine) among groups (IB), (IV) and (IIB)

		Group (IB)	Group (IV)	Group (IIB)	Test value•	P-value	Sig.
		n = 10	n= 10	n= 10			
Urea (mg/dl)	Mean ± SD	24.30 ± 1.64	24.48 ± 4.80	24.37 ± 1.45	0.009	0.991	NS
	Range	21 – 26	16 – 31	22 – 26.1			
Creatinine (mg/dl)	Mean ± SD	0.82 ± 0.04	0.84 ± 0.06	0.82 ± 0.05	0.630	0.540	NS
	Range	0.75 – 0.87	0.77 – 0.96	0.75 – 0.89			

Group (IB): (Negative Control group), Group (IIB): (Positive control group), Group (IV): (dependence group), n: number; SD: standard deviation; P-value >0.05: Non significant (NS); P-value <0.05: Significant (S); P-value< 0.01: highly significant (HS). •: One Way ANOVA test

Table (4): One way ANOVA to compare cardiac enzymes (CPK total, CK-MB and troponin) among groups (IB), (IV) and (IIB)

		Group (IB) n= 10	Group (IV) n= 10	Group (IIB) n= 10	Test value•	P-value	Sig.
CPK (U/L)	Mean ± SD	175.00 ± 8.67	3211.50 ± 268.71	189.70 ± 11.20	1267.293	0.000	HS
	Range	160 – 185	2975 – 3870	175 – 210			
CK-MB (U/L)	Mean ± SD	20.70 ± 1.95	1144.98 ± 174.11	20.90 ± 2.73	416.753	0.000	HS
	Range	18 – 23	956.8 – 1500	18 – 25			
Troponin	Negative	10 (100.0%)	10 (100.0%)	10 (100.0%)	NA	NA	NA

Group (IB): (Negative Control group), Group (IIB): (Positive control group), Group (IV): (dependence group), n: number; SD: standard deviation; CPK: creatine phosphokinase; CK-MB: creatIne kinase MB; P-value >0.05: Non significant (NS) P-value >0.05: Non significant (NS); P-value <0.05: Significant (S); P-value< 0.01: highly significant (HS), not applicable (NA), •: One Way ANOVA test

Table (5): post hoc statistical analysis to compare between three groups (negative IB and positive control IIB) versus dependence group (IV) as regards CPK-total and CPK-MB

	Post Hoc analysis by LSD		
	Group (IB) Vs Group (IV)	Group (IB) Vs Group (IIB)	Group (IIB) Vs Group (IV)
CPK	0.000	0.834	0.000
CK-MB	0.000	0.996	0.000

CPK: creatine phosphokinase; CK-MB: creatine kinase-MB; Vs: versus; LSD: least significant difference, P-value >0.05: Non significant, P-value <0.05: Significant, P-value< 0.01: highly significant

The effect of Strox on the histopathology of the heart (Figure 1):

Sections of the heart of both control groups (I&II) that showed almost similar normal histological structure (Figure 1a). In subgroup IIIA (1/3 LD50) cardiomyocytes were enlarged with homogenous acidophilic cytoplasm and congested blood capillaries in between (Figure 1b). In subgroup IIIB (2/3 LD50) most cardiomyocytes showed loss of striation and dark acidophilic sarcoplasm, however, few muscle fibers were massively dilated with homogenous acidophilic sarcoplasm. Congested dilated blood vessels appeared in between muscle fibers (Figure

1c). In subgroup IIIC (LD50) (sections from survived rats) showed cardiomyocytes were severely affected appearing fragmented with pyknotic nuclei. The blood vessels in between cardiomyocytes were filled with homogenous acidophilic materials entrapping RBCs (Figure 1d). In group IV (Dependence group) cardiomyocytes were thinned out, discontinuous and widely separated with extravasated blood (Figure 1e).

The effect of Strox on the histopathology of liver (Figure 2):

Sections of the liver of both control groups (I&II) showed normal architecture (Figure 2a). In subgroups IIIA, IIIB, IIIC, most hepatocytes showed cytoplasmic vacuolization, while others were ballooned with degenerated or absent nuclei (Figure 2b-2d). In subgroup IIIC (LD50) (sections from survived rats), peripheral hepatocytes beneath the capsule appeared vacuolated with hyperchromatic nuclei. Some deeper hepatocytes were ballooned, while others were variable in size and shape and were widely separated from each other (Figure 2d). In group IV (dependence group), areas of hepatocytes loss were detected beneath a thickened hepatic capsule. These areas were infiltrated with extravasated RBCs and mononuclear cellular infiltration (Figure 2e).

The effect of Strox on the histopathology of kidney (Figure 3):

kidney of the control groups (I&II) showed normal histological architecture (Figure 3a). Vacuolations of the epithelial lining of renal tubules appeared in subgroup IIIA (1/3LD50) and in subgroup IIIB (2/3LD50) and was more severe in group IV (dependence group) (Figure 3b, 3c and 3e respectively). Shrunken glomerular capillaries with widening of Bowman's space was seen in subgroup IIIB (2/3LD50) and subgroup IIIC (LD50) (sections from survived rats) with detachment of few epithelial cells lining the renal tubules in some areas while other epithelial cells showed pyknotic nuclei (Figure. 3c and 3d). These findings were more severe in group IV (Dependence group) (Figure 3e). In subgroup IIIC (LD50) (sections from survived rats) most of the renal tubules showed casts in their lumen (Figure 3d).

The effect of Strox on the histopathology of cerebellum (Figure 4):

The control groups (I&II) showed the cerebellar cortex was formed of 3 layers; superficial molecular layer, middle purkinje cell layer, and an inner granular layer (Figure 4a). All experimental groups showed an apparent decrease in the number of cells in the outer molecular layer and purkinje cell layer (Figure 4b-4e), however, degeneration of purkinje cells appeared in subgroups IIIB, IIIC and group IV (Figure 4c-4e). Moreover, in subgroup IIIC (sections from survived rats); there was separation between the molecular and Purkinje cell layer (Figure. 4d). In subgroups IIIB, IIIC and group IV a decrease in the thickness and cell number of the granular layer was detected with degeneration of cells in subgroup IIIC (Figure 4c-4e).

The effect of Strox on the histopathology of lung (Figure 5):

The lung of the control groups (I&II) showed normal histological structure (Figure 5a). All experimental groups showed thickened alveolar septa that were infiltrated with inflammatory cells, hemorrhage with hemosiderin granules and homogenous acidophilic materials (fig. 5b-5e). In subgroup IIIB (2/3LD50), lymphocytic aggregations appeared in the inter-alveolar septa (fig. 5c). In subgroup IIIC (LD50) (sections from survived rats), some alveolar spaces were obliterated and filled with inflammatory cells and RBCs (Figure 5d). In group IV (Dependence group), many alveolar spaces were filled with hyaline pale acidophilic homogenous material (Figure 5e)

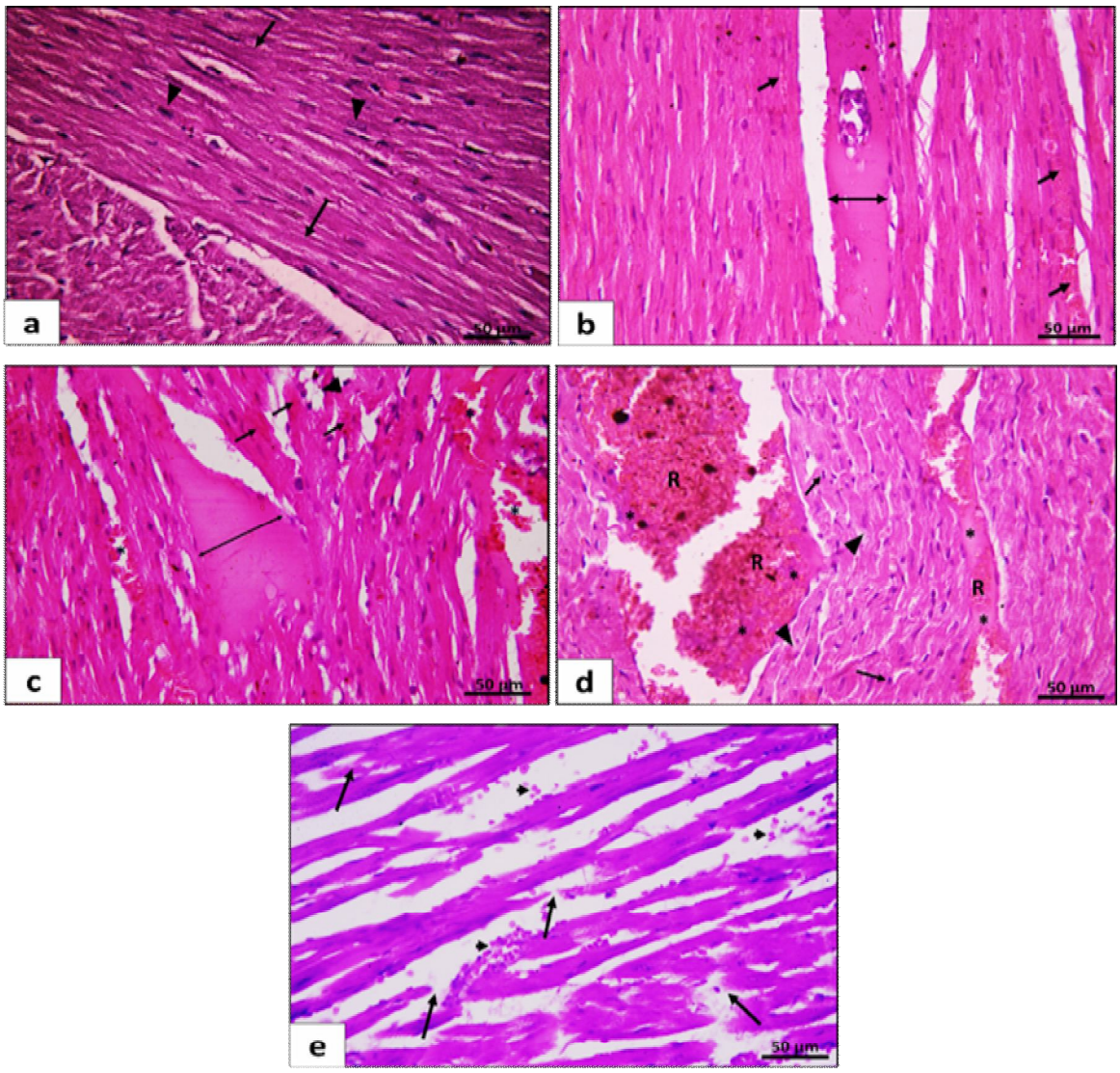

Fig. (1): Effect of Strox on the histopathology of heart. (a) Heart of the control groups (I&II) showing branching and anastomosing cardiac muscle fibers having acidophilic sarcoplasm showing transverse striations (↑). Their nuclei are oval vesicular and central in position (▲). **(b) Subgroup IIIA (1/3LD50 of Strox)** showing a cardiomyocyte appears enlarged with homogenous acidophilic cytoplasm (double headed arrow). Congested blood capillaries can be noticed in between cardiac muscle fibers (↑). **(c) Subgroup IIIB (2/3LD50 of Strox)** showing some cardiac muscle fibers exhibit loss of striation and appear with dark acidophilic sarcoplasm (↑), while other fibers were massively dilated with homogenous acidophilic sarcoplasm (double headed arrow). Vacuolated spaces are seen in between muscle fibers (▲). Blood vessels in between cardiac muscle appear dilated and congested (*). **(d) Subgroup IIIC (LD50 of Strox)** showing fragmented cardiac muscle fibers (arrowheads) with pyknotic nuclei (arrow). The blood vessels in between cardiac muscles are congested (*) and interrupted (R). **(e) Group IV (Dependence group)** showing the cardiac muscle fibers are widely separated from each other with extravasated blood (arrowheads). The cardiomyocytes appear thinned out and discontinuous in some areas (↑). **(H&E x400).**

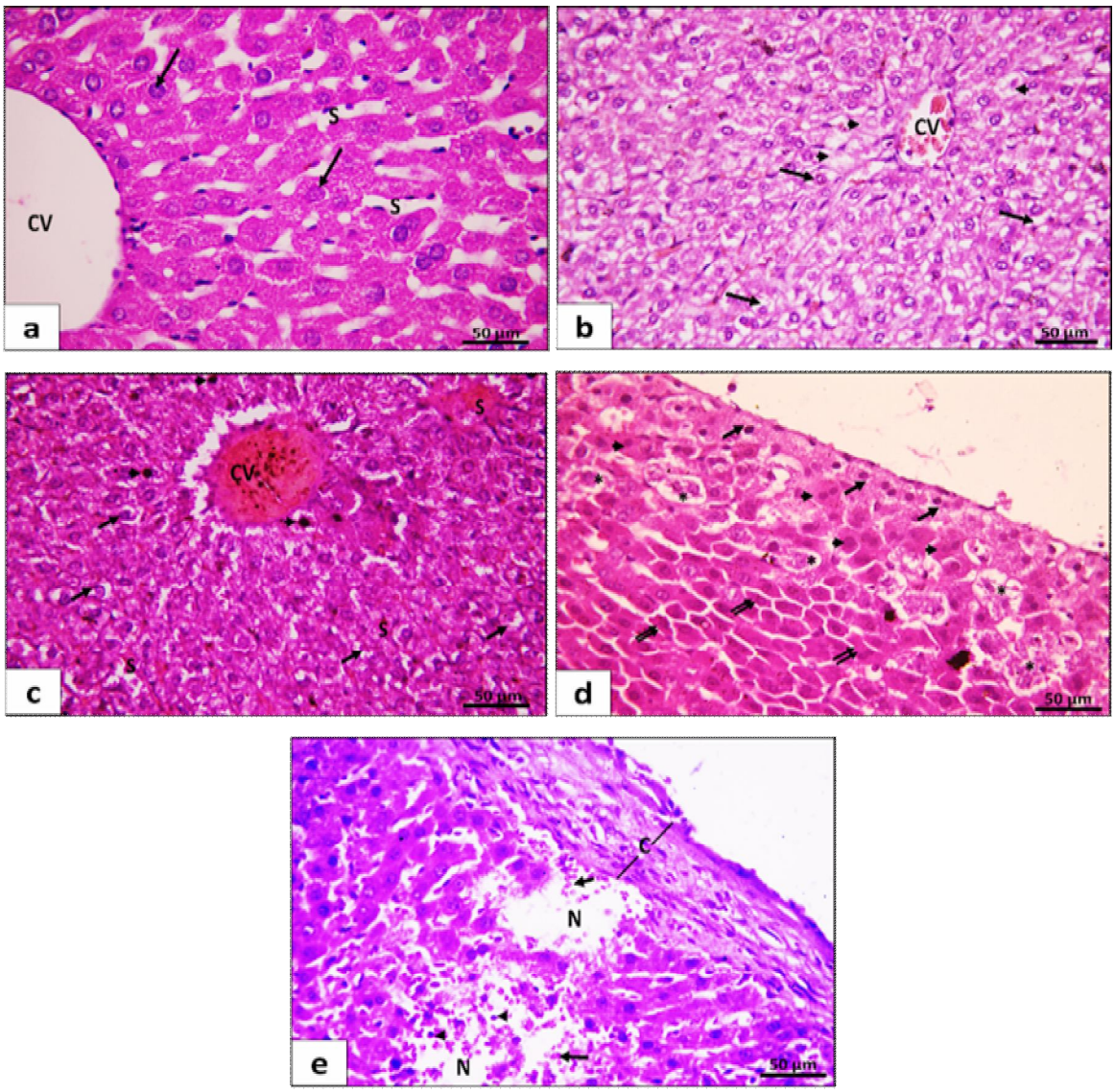

Fig. (2): Effect of Strox on the histopathology of liver. (a) Liver of the control groups (I&II) showing normal architecture with orderly arranged hepatocytes in cords radiating from the central vein (CV) with in between hepatic blood sinusoids (S). Hepatocytes are polygonal in shape having acidophilic granular cytoplasm and vesicular nuclei (↑). **(b) Subgroup IIIA (1/3LD50 of Strox)** showing most of the hepatocytes exhibit cytoplasmic vacuolization with vesicular nuclei (↑). Other hepatocytes around the congested central veins (CV) appear ballooned with degenerated or absent nuclei (arrowheads). **(c) Subgroup IIIB (2/3LD50 of Strox)** showing hepatocytes display cytoplasmic vacuolization (↑) with vesicular nuclei, while others appear with hyperchromatic nuclei (arrowheads). The central vein (CV) as well as blood sinusoids (S) are congested. **(d) Subgroup IIIC (LD50 of Strox)** showing some hepatocytes lying beneath the capsule appear vacuolated with hyperchromatic nuclei (↑). Some deeper hepatocytes are ballooned (*), others exhibit variability in size and shape and are widely separated from each other (↑↑). **(e) Group IV (Dependence group)** showing areas of loss of hepatocytes (N) beneath a thickened hepatic capsule (C) and infiltrated with RBCs (↑) and inflammatory cells (arrowheads). **(H&E x400).**

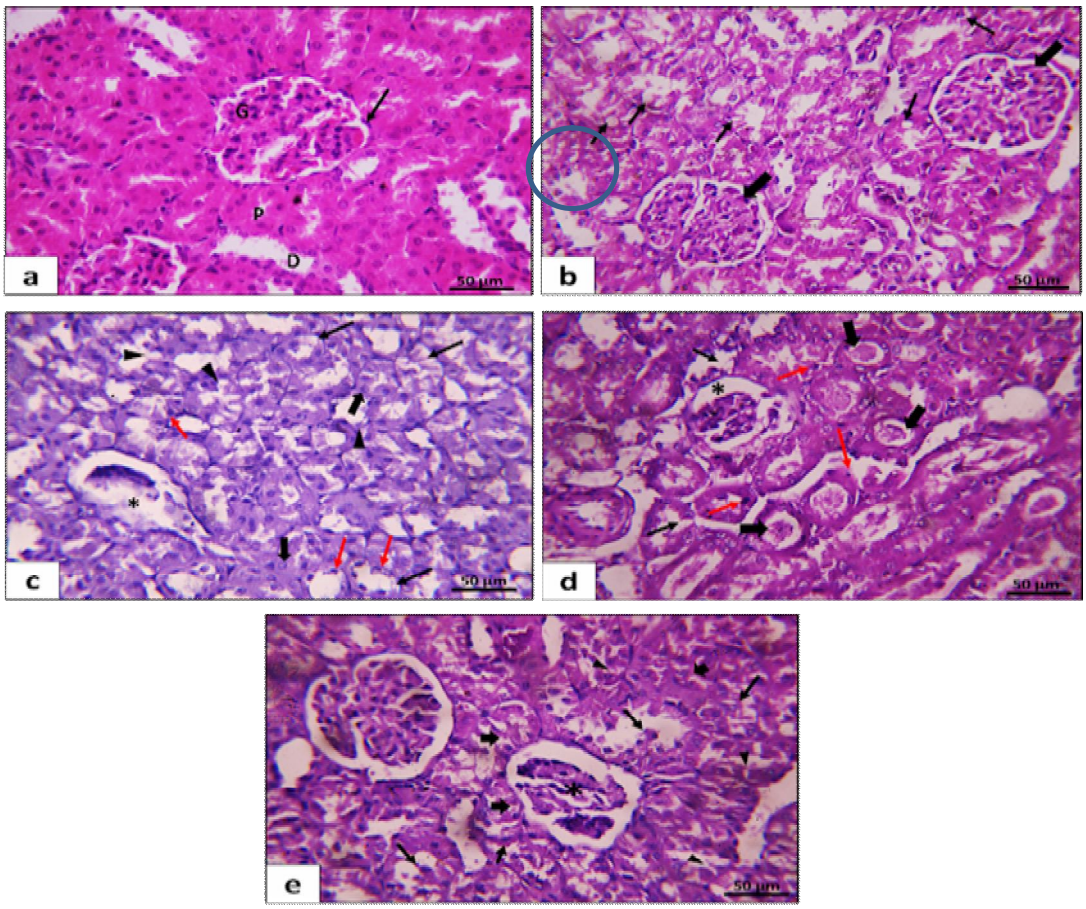

Fig. (3): Effect of Strox on the histopathology of kidney. (a) Kidney of the control groups (I&II) showing renal cortex is formed of renal corpuscles lined by Bowman's capsule (↑), the glomerulus (G) appears as a large cellular mass enclosing glomerular capillaries. Proximal convoluted tubules (P) are having narrow star shaped lumen and are lined by acidophilic cuboidal cells with apical brush border. The distal convoluted tubules (D) are seen having wider lumen. **(b) Subgroup IIIA (1/3LD50 of Strox)** showing the epithelial lining of both the proximal and the distal tubules show damaged and detached cells with pyknotic nuclei (↑). **(c) Subgroup IIIB (2/3LD50 of Strox)** showing a renal corpuscle displays shrunken glomerular capillaries with widening of Bowman's space (*). The surrounding renal tubules have vacuolations of their cytoplasm (black arrow) and loss of few epithelial cells denoted by separation of epithelial cells enclosed within the same tubular loop (▲). Notice that most nuclei of the epithelial cells lining the tubules are deeply stained (red arrow) while only few nuclei are vesicular (Thick arrow). **(d) Subgroup IIIC (LD50 of Strox),** a renal corpuscle shows shrunken glomerular capillaries with widening of Bowman's space (*). Most of the surrounding renal tubules show casts in their lumen (Thick arrow). The epithelial cells lining the tubules show loss of some cells (Black arrow), and shrunken pyknotic nuclei in some tubules (Red arrow). **(e) Group IV (Dependence group),** renal cortex showing shrunken glomerulus inside a renal corpuscle (*). The epithelial lining of the surrounding renal tubules shows vacuolation of their cytoplasm in most cells with many pyknotic nuclei (thick arrow). Some cells are detached in some tubules (↑) while other cells are widely separated in other tubules (arrowheads) **(H&E x400).**

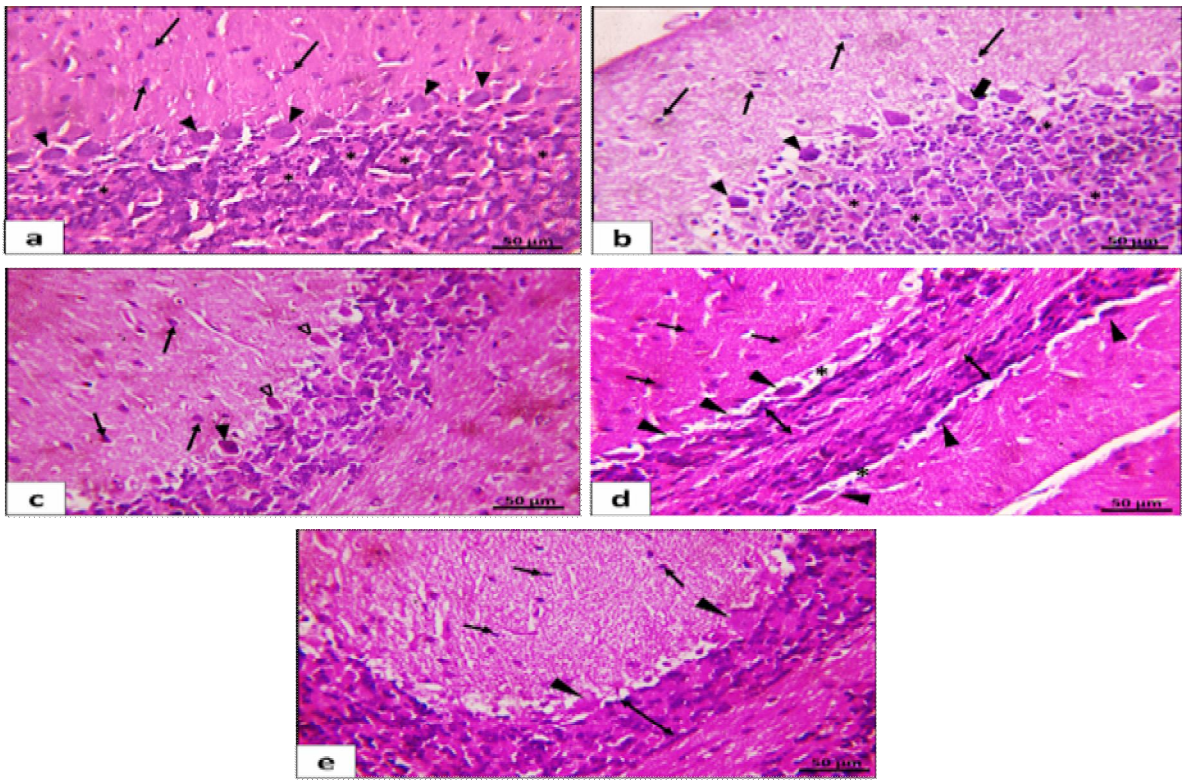

Fig. (4): Effect of Strox on the histopathology of cerebellum. (a) The control groups (I&II) showing the cerebellar cortex formed of 3 layers; superficial molecular layer containing nuclei of outer stellate cells and basket cells (↑); middle purkinje cell layer formed of a single layer of purkinje cells arranged in a single raw having a large flask shaped cell body and a large vesicular nucleus (arrowheads); an inner granular layer that lies on the surface of the cerebellar white matter formed of tightly packed nuclei of granule cells and Golgi cells separated by non-cellular spaces of cerebellar islands (*). **(b) Subgroup IIIA (1/3LD50 of Strox)**, there is an apparent decrease in the number of the nuclei of the outer stellate and basket cells in the superficial molecular layer (↑). In the middle Purkenji cell layer, Purkenji cells are apparently decreased in number in comparison to the control group. Some Purkenji cells have large flask shaped cell body with vesicular nuclei comparable to the control (thick arrow), however, few cells are distorted and show deep acidophilic cytoplasm and dark pyknotic nuclei (▲). The inner granular layer is formed of tightly packed nuclei of granule and Golgi cells separated by non-cellular cerebellar islands. **(c) Subgroup IIIB (2/3LD50 of Strox),** there is an apparent decrease in the number of the nuclei of the outer stellate and basket cells in the superficial molecular layer (↑). In the middle Purkenji cell layer, Purkenji cells are widely spaced with apparent decrease in their number compared to the control group, their cell bodies are distorted and shrunken. Their nuclei are either dark pyknotic (▲) or absent (Δ). The inner granular layer shows apparent decrease in its thickness and in the number of nuclei of granule and Golgi cells compared to the control and 1/3 LD 50. **(d) Subgroup IIIC (LD50 of Strox),** there is an apparent decrease in the number of the nuclei of the outer stellate and basket cells in the superficial molecular layer (↑). The outer molecular layer is separated from the underlying Pukenji cell layer by a narrow space (*) containing few Purkenji cells. Purkenji cells are distorted, widely spaced, and having dark pyknotic nuclei (▲). The inner granular layer shows apparent marked decrease in its thickness (↕) and in the number of nuclei and granule and Golgi cells which appear darkly stained compared to the other groups. **(e) Group IV (Dependence group),** superficial molecular layer shows apparent decrease in the amount nuclei of outer stellate cells and basket cells (↑); purkinje cells are markedly decreased in number with two degenerated cells (arrowheads); the inner granular layer shows apparent marked decrease in its thickness (↕) **(H&E x400).**

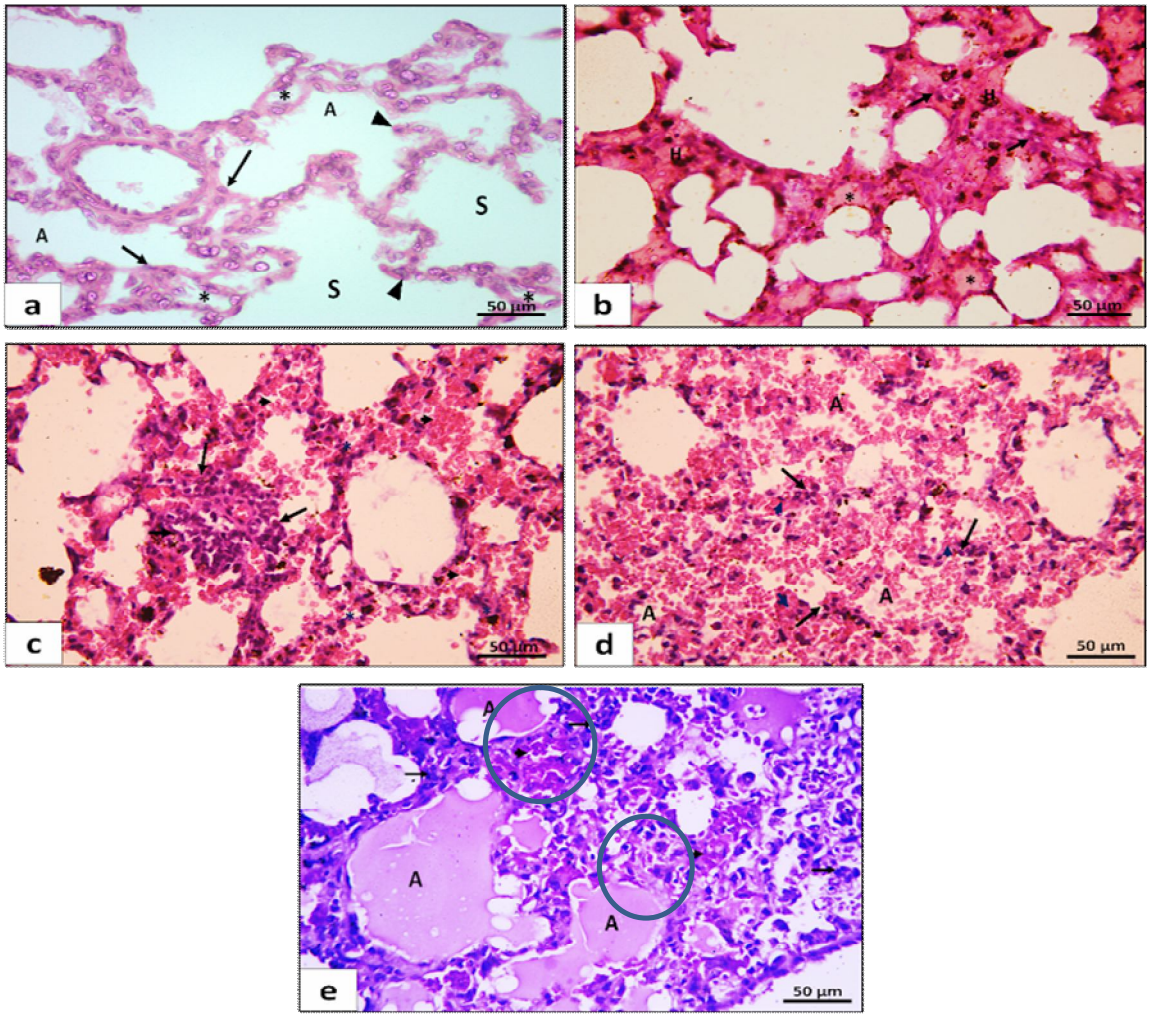

Fig. (5): Effect of Strox on the histopathology of lung. (a) The lung of the control groups (I&II) showing the alveoli (A) and the alveolar sacs (S) are lined with flattened type I pneumocytes (↑) and cuboidal type II pneumocytes (▲). The inter-alveolar septa are thin containing blood capillaries (*). **(b) Subgroup IIIA (1/3LD50 of Strox)** showing the inter-alveolar septa are thickened and infiltrated with inflammatory cells (↑), hemosiderin granules (H) and homogenous acidophilic materials (*). **(c) Subgroup IIIB (2/3LD50 of Strox)** showing the inter-alveolar septa with infiltrating inflammatory cells (*), extravasated blood (arrowheads) and lymphocytic aggregation (↑). **(d) Subgroup IIIC (LD50 of Strox)** showing inter-alveolar septa are thickened and heavily infiltrated with mononuclear inflammatory cells (↑) and extravasated blood (arrowheads). Some alveolar spaces are obliterated and filled with inflammatory cells and RBCs (A). **(e) Group IV (Dependence group)** showing many alveolar spaces are filled with hyaline pale acidophilic homogenous material (A). Inter-alveolar interstitium is heavily infiltrated by inflammatory cells and extravasated blood (↑). Dilated congested blood capillaries can be noticed (arrowheads) **(H&E x400).**

Discussion

Strox is a new psychoactive substance that has been spread among users in Egypt. According to Hussien et al. (2020) it is a blend of synthetic cannabinoids, various psychoactive substances, and herbal compounds. To our knowledge, no published articles have addressed Strox's histopathological or biochemical changes in various body organs. The current study investigated these changes due to Strox's acute toxic and dependence effects on the liver, kidney, lungs, brain, and heart.

Hussien et al. (2020) found increased CK-MB and troponin in patients with acute toxicity of synthetic cannabinoids, and attributed these cardiovascular effects to the sympathomimetic effects of voodoo components such as amphetamine, MDA, and synthetic cannabinoids, which are the leading cause of heart failure. In addition to causing arrhythmias, and myocardial ischemia, synthetic cannabinoids can also lead to cardiomegaly and dilated cardiomyopathy (Giorgetti et al., 2020; Simon et al., 2022). Moreover, patients with SC intoxication reported cardiotoxicity in the form of myocardial infarction, bradycardia, and prolonged QT interval (Kourouni et al., 2020).

The liver was markedly affected in the histopathology of both acute and dependence groups. The liver is the main organ responsible for the metabolism of most drugs and toxic substances. Amphetamine, 3, 4-Methylenedioxyamphetamine (MDA), MDMA, and synthetic cannabinoids, which are the main constituents of Strox, could be responsible for its hepatotoxicity (Hussien et al., 2020). The liver metabolizes these substances, producing toxic metabolites (Pontes et al., 2010). Payancé et al. (2013) reported that chronic use of MDMA can produce liver damage up to fibrosis. The current study found a correlation between elevated liver enzymes and liver affection in histopathology. Other studies also reported abnormal liver enzymes as the most common laboratory findings among synthetic cannabinoid users (Murat et al., 2018; Tawfik, 2021). In contrast to our study, Hussien et al. (2020) found normal liver enzymes in most of the studied patients.

In the current study, kidney affection occurred in both acute and dependence groups. Srisung et al. (2015) reported that common acute kidney injury occurred among users of synthetic cannabinoid with unknown pathophysiology. These synthetic cannabinoids are one of the main constituents of Strox (Hussien et al., 2020). However, the markedly increased CPK level in the dependence group suggests rhabdomyolysis as a potential cause of kidney affection. Normal renal function tests in the current study correspond to studies by Hussien et al. (2020) and Tawfik (2021), who found normal serum urea and creatinine in most of their studied patients with SC intoxication.

Strox also had an effect on the cerebellar cortex in both the acute and dependence groups. The effect on cannabinoid receptor type 1 (CB1), which is present with high densities in the cerebellum and significantly modulates GABA and glutamate neurotransmission, could explain the current findings (Castaneto et al., 2014). Moreover, Chase et al. (2016) and Seely et al. (2013) attributed the neurotoxic effect of SC to its content of multiple unstandardized constituents and possibly adulterants including its plant material effects during its production in the clandestine laboratories.

The neurological effects of SC were seen in patients as well, including seizures, agitation, and coma, as well as diffuse brain edema and loss of gray/white differentiation in brain CT (Kourouni et al., 2020).

A histopathological study of rat lungs in the acute toxicity group showed thickened inter-alveolar septa and mononuclear cellular infiltration. On the other hand, the dependence group's lungs were filled with hyaline, pale acidophilic homogenous material and had a lot of inflammatory cells and extravasated blood in the inter-alveolar interstitium, as well as a lot of congestion. The dominant changes in the lung tissue are consistent with Mousa et al. (2021). Moreover, Alhadi et al. (2013) reported diffuse pulmonary infiltrates in the histopathological examination of bronchial and alveolar tissues of a chronic user of synthetic cannabinoids (SC). Zawatsky et al. (2020) said that SC's effects on the lungs were caused by its binding to cannabinoid receptor 1 (CB1R) in the lungs, which led to lung damage, inflammation of the alveoli, and scarring. We assumed that the hyaline exudate filling the alveoli and the marked cellular infiltration in the lung sections represent early-stage ARDS (Acute Respiratory Distress Syndrome), a condition often observed in chronic SC users requiring mechanical ventilation (Alhadi et al., 2013; Yamanoglu et al., 2018).

Schmid et al. (2003) found that SC caused respiratory depression in rats and attributed this to the increased bronchial airway resistance effect **of** the CB1 receptor on peripheral chemo-baroreceptors by an unknown mechanism. Yamanoglu et al. (2018) confirmed the same respiratory depressant effect through blood gas analysis.

Conclusion

The current study concluded that Strox has many toxic effects on experimental animals after acute and chronic exposure. Strox toxicity, both acute and chronic, affected the structure of all examined organs to varying degrees. The altered biochemical results mirrored the affected structure, with the exception of the kidney.

Availability of data and material statement:

All data generated or analyzed during this study are included in this published article.

Conflict of interest: None

References:

Abass MA , Hassan MZ, Abd Elhaleem MR, et al. (2017) 'Acute toxicity of a novel class of hallucinogen "Voodoo" (Clinical and experimental study)', *Ain Shams Journal of Forensic Medicine and Clinical Toxicology*, 28(1), pp 62-71

Alhadi S, Tiwari A, Vohra R, et al. (2013) 'High times, low sats: Diffuse pulmonary infiltrates associated with chronic synthetic cannabinoid use', *J. Med. Toxicol.*, 9(2), pp.199-206.

Castaneto MS, Gorelick DA, Desrosiers NA, et al. (2014) 'Synthetic cannabinoids: epidemiology, pharmacodynamics, and clinical implications', *Drug Alcohol Depend.*, 144, pp.12-41.

DOI: 10.1016/j.drugalcdep.2014.08.005

Charan J and kantharia ND (2013) 'How to calculate sample size in animal studies?' *Journal of Pharmacology and Pharmacotherapeutics*, 4 (4), pp.303-306, DOI:10.4103/0976-500X.119726

Chase PB, Hawkins J, Mosier J, et al. (2016) 'Differential physiological and

behavioral cues observed in individuals smoking botanical marijuana versus synthetic cannabinoid', *Drugs. Clin. Toxicol. (Phila),* 54(1), pp.14-19.

Drury RA and Wallington EB (1980). '*Carlton's Histology Techniques'*. 5th edition. Oxford University Press, England; pp: 139-239

El-Masry M, and Abdelkader S. (2021). 'Clinical profile of designer drug "strox" intoxicated cases presented to poison control center ain shams university, Egypt from first of January 2017 to end of January 2018'. *Ain Shams J Forensic Med Clin Toxicol.*; 36(1), pp.98-105, DOI: 10.21608/AJFM.2021.138857

Giorgetti A, Busardò FP, Tittarelli R, et al. (2020). 'Post-Mortem toxicology: A systematic review of death cases involving synthetic cannabinoid receptor agonists', *Front Psychiatry*, 25(11), pp.464.

Hussien R, Ahmed S, Awad H, et al. (2020). 'Identification of "Voodoo": An emerging substance of abuse in Egypt', *Int. J. Environ. Anal. Chem.*, pp 1–13.

Kourouni I, Mourad B, Khouli H, et al. (2020). 'Critical illness secondary to synthetic cannabinoid ingestion', *JAMA Netw Open.*; 3(7): e208516.

Loschner A, Cihla A, Jalali F, et al. (2011). 'Diffuse alveolar hemorrhage: add "greenhouse effect to the growing list'. *Chest*; 140(4), pp.149A.

Luethi D, and Liechti M (2020) 'Designer drugs: mechanism of action and adverse effects', *Archives of Toxicology*, 94, pp.1085–1133.

Mousa RE, Gebril SM, Masoud KMM, et al. (2021). 'Acute toxic effects of AB-CHMINACA on lung, heart and liver: An experimental pilot study', *Ain Shams Journal of Forensic Medicine and Clinical Toxicology*; 37, pp.128-135.

Murat Y, Nazlı T, Handan Y et al. (2018) 'Socio-demographic and clinical characteristics of synthetic cannabinoid users in a large psychiatric emergency department in Turkey', *J. Addict. Dis*., 37(3-4), pp.259-267.

Payancé A, Scotto B, Perarnau JM, et al. (2013) 'Severe chronic hepatitis secondary to prolonged use of ecstasy and cocaine', *Clin. Res. Hepatol.Gastroenterol.*, 37(5), pp.109-113.

Pontes H, de Pinho PG, Fernandes E, et al. (2010) 'Metabolic interactions between ethanol and mdma in primary cultured rat hepatocytes' *Toxicology*; 270 (2-3)pp.150–157.

Schmid K, Niederhoffer N, Szabo B (2003) 'Analysis of the respiratory effects of cannabinoids in rats', *Arch. Pharmacol.*, 368(4), pp.301.

Seely KA, Patton AL, Moran CL, et al. (2013) 'Forensic investigation of K2, Spice, and "Bath Salt" commercial preparations: A three-year study of new designer drug products containing synthetic cannabinoid, stimulant, and hallucinogenic compounds', *Forensic Sci. Int*., 233(1-3), pp.416-422.

Simon G, Tóth D, Heckmann V,et al. (2022). 'Lethal case of myocardial ischemia following overdose of the synthetic cannabinoid ADB-FUBINACA', *Legal Medicine*, 54 (144), pp. 102004.

Sobh H and Sobh Z. (2018). 'Strox: (Novel synthetic cannabinoids) in Egypt: medical and legal challenges', *Arab Journal of Forensic Sciences and Forensic Medicine*, 2(1), pp. 57-60.

Srisung W, Jamal F, Prabhakar S. (2015). 'Synthetic cannabinoids and acute kidney injury' *Proc. (Bayl Univ Med Cent),* 28(4), pp.475-477.

Tawfik HM (2021). 'Strox: A 3-year study of intoxicated cases admitted to poison control center Ain Shams University Hospitals', *Ain Shams Journal of Forensic Medicine and Clinical Toxicology*, 37, pp.1-7.

Wilson-Hohler M, Fathy WM and Mozayani A (2016). 'How present synthetic cannabinoids can help predict symptoms in the future', *MOJ Toxicol*., 2(1), pp.18-24

Yamanoglu A, SCakmak S, Yamanoglu NGC et al. (2018). 'A new side effect of synthetic cannabinoid use by the bucket (waterpipe) method: Acute respiratory distress syndrome (ARDS)', *Turkish Journal of Emergency Medicine*, 18(1), pp.42-44.

Zawatsky CN, Abdalla J, Cinar R (2020). 'Synthetic cannabinoids induce acute lung inflammation via cannabinoid receptor 1 activation', *ERJ Open Res*., 6(3), pp.00121-2020.